

Analyzing Oscillators Using Multitime PDEs

Onuttom Narayan and Jaijeet Roychowdhury

Abstract—Oscillators are often difficult to analyze or simulate, because they generate waveforms that can span a range of widely separated time scales. We present a general oscillator formulation that separates slow and fast dynamics without approximations, and captures amplitude and frequency modulation in a natural and compact manner. To handle frequency-modulation effectively, we make use of a novel concept, *warped time*, within a multitime partial differential equation framework. The equations incorporate an explicit time-varying frequency variable that matches intuitive notions of changing frequency in a frequency-modulated signal. The formulation is useful for both hand analysis and numerical simulation.

Index Terms—Frequency modulation (FM), multitime partial differential equation (MPDE).

I. INTRODUCTION

OSCILLATORS are ubiquitous in nature and can be found in a variety of physical systems. They are important in engineering and communications; for example, voltage-controlled oscillators (VCOs), phase-locked loops (PLLs), lasers, etc., abound in wireless and optical systems. When driven (or forced) by external signals, oscillators can exhibit complex dynamics, such as frequency modulation (FM), entrainment or injection locking, period multiplication and chaos. Despite their universality, understanding of such systems is far from complete, and it is often difficult to analyze or predict the response of a general autonomous system in a satisfactory and reliable manner.

In this paper, we present a new approach for analyzing frequency and amplitude modulation in oscillators. The approach is a generalization of a recent multiple-time scale analytical formulation, the multitime partial differential equation (MPDE) [1], [2] for nonoscillatory dynamical systems. The MPDE is not well suited to analyzing FM, particularly FM with high modulation indices—a phenomenon that occurs in oscillatory systems and is often used in applications. In this paper, we dynamically rescale (“warp”) the time axis to make the undulations of the FM signal uniform, therefore easy to represent compactly as periodic or quasi-periodic¹ functions. The rescaling function is not known *a priori*, but becomes an unknown function that is solved for along with the rest of the system to yield a time-varying local frequency for the oscillator. These concepts

are embedded within the framework of multiple time scale analysis of dynamical systems. This achieves a symbolic separation of the (typically slow) rates of FM and amplitude modulation (AM) from the (much faster) nominal oscillation rate. The resulting formulation is a multi-time partial-differential equation in warped and unwarped time scales, together with a mapping between multi-time and single-time functions. We dub this the **Warped MPDE (WaMPDE)**.

The WaMPDE can be directly applied to oscillators for which simple closed-form equations are available (e.g., the neoclassical equations for lasers [4]) in order to obtain useful qualitative and quantitative results. It can also be used to derive efficient numerical methods for simulating oscillators described by large or complicated equation systems, that are not amenable to hand analysis. This is possible because the equivalence between the WaMPDE and the original dynamical equations of the oscillator does not rely on approximations. Numerical computations using the WaMPDE can be performed using time-domain or frequency-domain methods, or combinations. In particular, existing codes for the MPDE, or steady-state simulation methods like shooting or harmonic balance, can be modified easily to perform WaMPDE-based calculations. If iterative linear-equation solvers (e.g., [5]–[8]) are used for underlying computations, large dynamical systems can be simulated efficiently.

Most previous works on oscillators start from single-time differential equation descriptions. Works geared toward practical oscillator design typically linearize the oscillator equations (e.g., [9]–[12]). This is a very approximate approach that cannot predict important qualitative properties of oscillators (such as amplitude stability, since nonlinearity is essential for orbitally stable limit cycles [13]). Nevertheless, linearization does provide useful partial insights into oscillator operation, such as the well-known Barkhausen oscillation criterion. Nonlinear analyzes (e.g., [14]–[16], [13], [17]) have largely been of oscillators with simple closed-form differential equations, such as the van der Pol equation [18]. Many studies (see, e.g., [19], [20]) have focused on chaos and subharmonic generation in simple nonlinear oscillators, such as the Lorenz attractor [21] and Chua’s circuit [22]. Comparatively little attention appears to have been paid to the dynamics of phenomena like FM-type quasi-periodicity, despite their widespread application.

A previous analytical technique with similarities to our present approach is the multiple-variable expansion procedure (e.g., [23], [24]) that relies on asymptotic expansions. This is intrinsically a perturbation approach, useful mainly for simple harmonic oscillators with small nonlinear perturbation terms and without external forcing. Another technique somewhat related to the present work is the slowly-varying envelope approximation (SVEA) (e.g., [4]), an analytical approach that is used to derive approximate equations for slowly-varying quantities from closed-form oscillator differential equations (ODEs). The WaMPDE can be considered a generalization of

Manuscript received April 15, 2001; revised November 14, 2001 and April 10, 2002. This paper was recommended by Associate Editor M. Gilli.

O. Narayan is with the Tata Institute of Fundamental Research, Bangalore 560012, India.

J. Roychowdhury is with the Electrical and Computer Engineering Department, University of Minnesota, Minneapolis, MN 55455-0154 USA.

Digital Object Identifier 10.1109/TCSI.2003.813976

¹The term *quasi-periodic* is defined in, e.g., [2], [3]. In this paper, we will use the looser interpretation mentioned in Section II.

the SVEA; in fact, the SVEA can be derived from the WaMPDE by expanding the oscillation time scale in a Fourier basis and applying approximations.

For the design and verification of practical oscillators, computer simulation is often the only choice as simple closed-form equations are often unavailable. Unfortunately, simulation of oscillators using time-stepping differential equation solvers such as SPICE [25], [26] presents unique difficulties absent in nonautonomous systems. A fundamental problem is the intrinsic phase-instability of oscillators, i.e., the absence of a time reference. As a result, numerical errors grow and phase error increases unboundedly in the course of numerical ODE solution, and this problem is exacerbated in large systems of equations. For unforced oscillators in periodic steady state, boundary-value methods such as shooting [20], [27]–[29], and harmonic balance [24], [30]–[35] can be used to obtain both the time period and the steady-state solution. Neither shooting nor harmonic balance can be applied, however, to forced oscillators with FM-quasi-periodic responses, as they require an impractically large number of time steps or variables. In practice, the separation of the time scales is often reduced artificially to make the problem tractable, but such ad-hoc approaches can lead to qualitatively misleading results. WaMPDE-based numerical methods can efficiently simulate large systems with amplitude and FM in the presence of widely separated signal rates and strong nonlinearities. In addition, they alleviate the phase-error-accumulation problem greatly by decoupling the integration of the phase error completely from the solution of the rest of the system. Further generalizations of the WaMPDE, potentially applicable to more complex oscillatory systems, are presented in Appendix.

Previous efforts to generalize the MPDE to autonomous systems [36] used nonrectangular boundaries in the multiple time domain to capture frequency variation. This approach is however limited to oscillations that eventually become periodic, and cannot, for instance, accommodate FM-quasi-periodicity (see the Appendix).

The remainder of the paper is organized as follows. Section II contains a discussion of multiple time scales and warped time, the use of which to develop the WaMPDE is presented in Section III. In Section IV, numerical methods based on the WaMPDE are applied to simulate a VCO and the results compared against time-stepping simulation.

II. WARPED TIME AND MULTIPLE TIME SCALES

In this section, we introduce several preliminary concepts in order to motivate the steps in Section III. We first review why it is advantageous to use two or more time scales for analyzing quasi-periodic signals, using AM signals for illustration. Then, we show that although FM signals can be quasi-periodic, the multitime approaches that work for AM (or immediate extensions thereof) do not confer the same advantages. Next, we introduce the concept of warped time and show how it can be used to remedy the situation for FM. We discuss the important issue of ambiguities in the concept of local frequency, and show how to obtain a useful definition that is consistent with intuition.

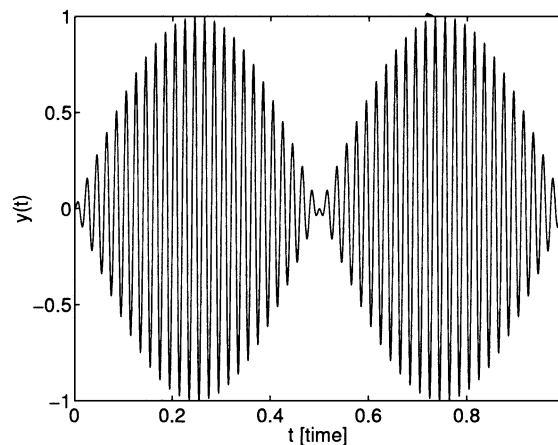


Fig. 1. Example of two-tone quasi-periodic signal $y(t)$.

Consider the waveform $y(t)$ shown in Fig. 1, a simple two-tone quasi-periodic² signal given by

$$y(t) = \sin\left(\frac{2\pi}{T_1}t\right) \sin\left(\frac{2\pi}{T_2}t\right), \quad T_1 = 0.02 \text{ s}; \quad T_2 = 1 \text{ s}. \quad (1)$$

The two tones are at frequencies $f_1 = 1/T_1 = 50$ Hz and $f_2 = 1/T_2 = 1$ Hz, i.e., there are 50 fast-varying sinusoids of period $T_1 = 0.02$ s modulated by a slowly-varying sinusoid of period $T_2 = 1$ s. Such multirate waveforms, i.e., with two or more “components” varying at widely separated rates, arise in many situations.

For $y(t)$, we have a compact closed-form representation in the form of (1). However, for most differential-algebraic equation (DAE) descriptions of oscillators, it is usually not possible to find closed-form expressions for their waveforms, yet compactness of representation is valuable for both analytical and numerical purposes. We will measure compactness of representation through the number of samples from which the signal can be reconstructed, to within a desired accuracy. This measure is not only directly useful for numerical purposes, but because of its links to bandwidth through Shannon’s sampling theorem, is also valuable for analytical purposes.

For $y(t)$ above, the samples need to be spaced closely enough to represent each rapid undulation accurately. If each fast sinusoid is sampled at n points, the total number of time steps needed for one period of the slow modulation is $n(T_2/T_1)$. To generate Fig. 1, 15 points were used per sinusoid, hence the total number of samples was 750. This number can be much larger in applications where the rates are more widely separated, e.g., separation factors of 1000 or more are common in electronic circuits. Also, while the particular $y(t)$ in (1) can be compactly represented in the frequency domain with only two Fourier components, the same is not true for, e.g., the product of a sine wave and a square wave. Hence frequency-domain representations do not, in general, solve the problem of inefficient representation of multi-rate signals.

²Although this signal is strictly periodic (with period 1s), its significance is that it can be written as $y(t) = \hat{y}(t, t)$, where \hat{y} is periodic in each of its arguments [e.g., as in (2)]. We will use the term *quasi-periodic* throughout this paper for any such signals, without insisting that the periods of \hat{y} be mutually incommensurate (which is the strict definition).

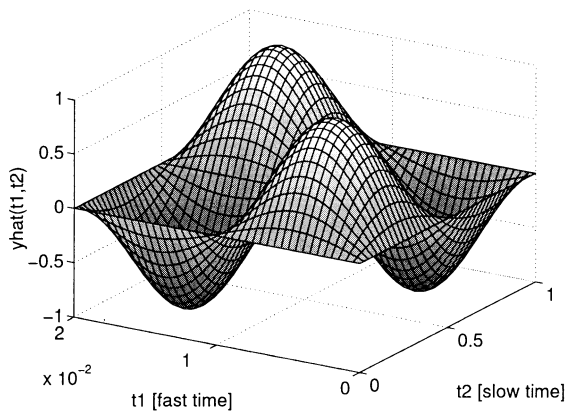


Fig. 2. Corresponding two-periodic bivariate form $\hat{y}(t_1, t_2)$.

Now consider a multivariate representation of $y(t)$, obtained as follows: for the “fast-varying” parts of $y(t)$, t is replaced by a new variable t_1 ; for the “slowly-varying” parts, by t_2 . The resulting function, now of two variables, is denoted by $\hat{y}(t_1, t_2)$

$$\hat{y}(t_1, t_2) = \sin\left(\frac{2\pi}{T_1}t_1\right) \sin\left(\frac{2\pi}{T_2}t_2\right). \quad (2)$$

Note that $\hat{y}(t_1, t_2)$ is periodic with respect to both t_1 and t_2 , i.e., $\hat{y}(t_1 + T_1, t_2 + T_2) = \hat{y}(t_1, t_2)$. The plot of $\hat{y}(t_1, t_2)$ on the rectangle $0 \leq t_1 \leq T_1, 0 \leq t_2 \leq T_2$ is shown in Fig. 2. Because \hat{y} is biperiodic, this plot repeats over the rest of the t_1 - t_2 plane. Note also that $\hat{y}(t_1, t_2)$ does not have many undulations, unlike $y(t)$ in Fig. 1. Hence it can be represented by relatively few points, which, moreover, do not depend on the relative values of T_1 and T_2 , unlike Fig. 1. Fig. 2 was plotted with 225 samples on a uniform 15×15 grid—three times fewer than for Fig. 1. This saving increases with increasing separation of the periods T_1 and T_2 .

Note further that it is easy to recover $y(t)$ from $\hat{y}(t_1, t_2)$, simply by setting $t_1 = t_2 = t$, and using the fact that \hat{y} is biperiodic. Given any value of t , the arguments to \hat{y} are given by $t_i = t \bmod T_i$. When the time scales are widely separated, inspection of the bivariate waveform directly provides information about the slow and fast variations of $y(t)$ more naturally and conveniently than $y(t)$ itself.

The above discussion illustrates two important features: 1. the bivariate form can require far fewer points to represent numerically than the original quasi-periodic signal, yet 2. it contains all the information needed to recover the original signal completely. These concepts are the key to the MPDE approach [1], [2] for analyzing nonautonomous systems. The basic notion is to solve directly for the compact multivariate forms of a DAEs solution. To achieve this, the DAE is replaced by a closely-related PDE called the MPDE. By applying boundary conditions to the MPDE and solving it with numerical methods, the multivariate solutions are obtained efficiently. The univariate solution of the original DAE can be easily computed from the multivariate solution of the MPDE; often, however, information of interest can be obtained directly by inspecting the multivariate solution. We refer the reader to [2] for further details.

When the DAEs under consideration contain autonomous components, FM quasi-periodicity can be generated. FM

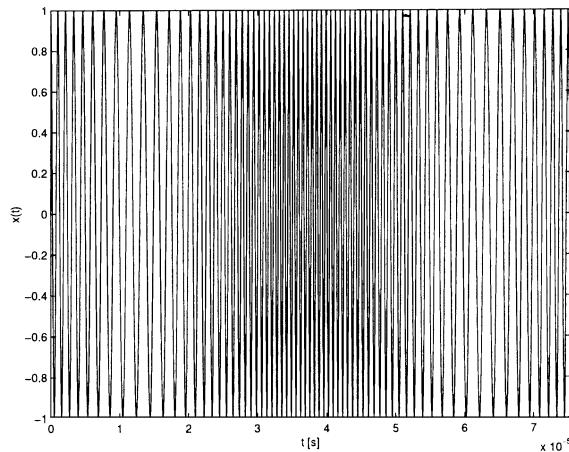


Fig. 3. FM signal.

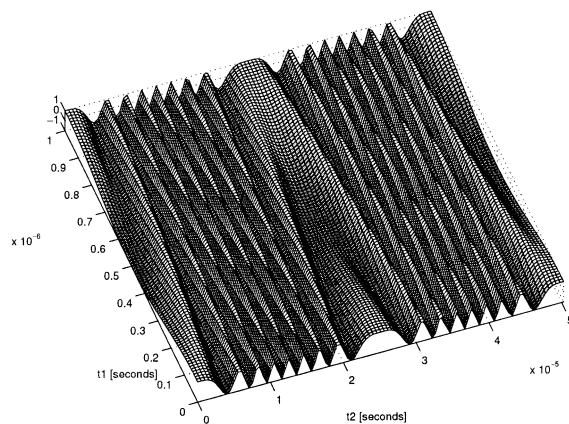


Fig. 4. \hat{x}_1 : unwarped bivariate representation of FM signal.

cannot, in general, be represented compactly as in Fig. 2. We illustrate the difficulty with an example. Consider prototypical FM signal

$$x(t) = \cos(2\pi f_0 t + k \cos(2\pi f_2 t)), \quad f_0 \gg f_2 \quad (3)$$

with instantaneous frequency

$$f(t) = f_0 - k f_2 \sin(2\pi f_2 t). \quad (4)$$

$x(t)$ is plotted in Fig. 3 for $f_0 = 1$ MHz, $f_2 = 20$ KHz, and modulation index $k = 8\pi$. Following the same approach as for (1), a bivariate form can be defined to be

$$\hat{x}_1(t_1, t_2) = \cos(2\pi f_0 t_1 + k \cos(2\pi f_2 t_2)), \quad \text{with } x(t) = \hat{x}_1(t, t). \quad (5)$$

Note that \hat{x}_1 is periodic in t_1 and t_2 , hence $x(t)$ is quasi-periodic with frequencies f_0 and f_2 . Unfortunately, $\hat{x}_1(t_1, t_2)$, illustrated in Fig. 4, is not a simple surface with only a few undulations like Fig. 2. When $k \gg 2\pi$, i.e., $k \approx 2\pi m$ for some large integer m , then $\hat{x}_1(t_1, t_2)$ will undergo about m oscillations as a function of t_2 over one period T_2 . In practice, k is often of the order of $(f_0/f_2) \gg 2\pi$, hence this number of undulations can be very large. Therefore, it becomes difficult to represent \hat{x}_1 efficiently by sampling on a two-dimensional grid. It is also clear, from Fig. 4, that representing (3) in the frequency domain

will require a large number of Fourier coefficients to capture the undulations.

A plausible approach toward resolving this representation problem is based on the intuition that FM is a slow change in the instantaneous frequency of a fast-varying signal. In the multivariate representation (2), the high-frequency component is the inverse of T_1 , the time period along the t_1 (fast) time axis. It is natural to hope, therefore, that FM solutions can be captured by making this time-period change along the slow time axis t_2 , i.e., change T_1 to a periodic function $T_1(t_2)$, itself periodic with period T_2 . Unfortunately, it can be shown ([2], and reproduced here in Appendix) that FM quasi-periodicity in a DAE cannot be captured by making T_1 a function of t_2 .³ It is easy to see qualitatively why this is the case. Although Figs. 2 and 4 show the signal over only one period in each of the two time directions, the bivariate form is actually periodic over the entire t_1 - t_2 plane. However, making the time-period T_1 a function $T_1(t_2)$ turns the rectangular domain $[0, T_1] \times [0, T_2]$ (of Figs. 2 and 4) into a nonrectangular domain of variable width (illustrated in Fig. 15 in the appendix). While it is possible to obtain a periodic function on the t_1 - t_2 plane by placing rectangular boxes side by side to tile the entire plane, it is obvious that this cannot be done with boxes of variable width.

The WaMPDE approach of this work resolves this problem by preserving the rectangular shape of the domain boxes, and bending the path along which $y(t)$ is evaluated away from the diagonal, so that its slope changes slowly. Since along the bent path $t_2 = t$, but t_1 is no longer equal to t , we refer to t_1 as a warped time scale. As mentioned in Section I, this stretches and squeezes the time axis differently at different times to even out the period of the fast undulations.

We illustrate this by returning to (3). Consider the following new multivariate representation:

$$\hat{x}_2(\tau_1, \tau_2) = \cos(2\pi\tau_1) \quad (6)$$

together with the warping function

$$\phi(\tau_2) = f_0\tau_2 + \frac{k}{2\pi} \cos(2\pi f_2\tau_2). \quad (7)$$

We now retrieve our one-dimensional (1-D) FM signal (i.e., (3)) as

$$x(t) = \hat{x}_2(\phi(t), t). \quad (8)$$

Note that both \hat{x}_2 and ϕ , given in (6) and (7), can be easily represented with relatively few samples, unlike \hat{x}_1 in (5). \hat{x}_2 and ϕ are plotted in Figs. 5 and 6. Note further that $\phi(t)$ is the sum of a linearly increasing term and a periodic term, hence its derivative is periodic. This periodic derivative is equal to the instantaneous frequency, given in (4), of $x(t)$. We will elaborate further on the significance of $(\partial\phi/\partial t)$ shortly.

It is apparent that there is no unique bivariate form and warping function satisfying (8)—for example, two representations \hat{x}_1 and \hat{x}_2 have already been given (the warping

³Nevertheless, Brachtendorf [36] has shown that this concept can be used to analyze transients in the special case of oscillators that eventually become T_1 periodic.

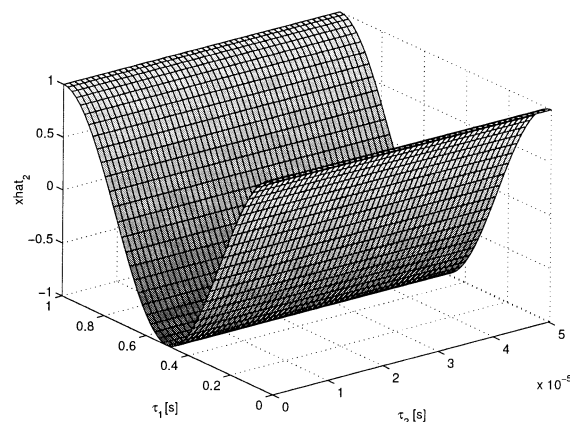


Fig. 5. \hat{x}_2 : warped bivariate representation of FM signal.

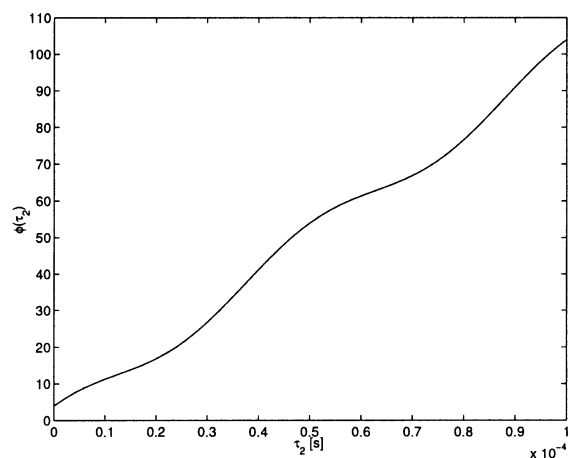


Fig. 6. $\phi(\tau_2)$: time warping function.

function for \hat{x}_1 is $\phi(t) = t$). More generally, any warping function can be chosen, but at the possible cost of a resulting bivariate representation that is not compact. To find an efficient bivariate representation, a crucial step in our approach is to avoid specifying the function $\phi(t)$ *a priori*, but to impose a smooth “phase” condition instead on the bivariate function, and use this to calculate ϕ . The phase condition can, for instance, require that the phase of the τ_1 -variation of the function should vary only slowly (or not at all) as τ_2 is changed. Alternatively, a time-domain condition on the bivariate function (or a derivative) can be specified. For example, consider the requirement that the τ_1 -derivative along the line $\tau_1 = 0$ be a slowly-varying function of τ_2

$$\frac{\partial \hat{x}_3(0, \partial\tau_2)}{\partial \tau_1} = -2\pi \sin(2\pi f_2\tau_2) \quad (9)$$

together with

$$\hat{x}_3(\phi_3(t), t) = x(t) = \cos(2\pi f_0 t + k \cos(2\pi f_2 t)). \quad (10)$$

As is easily verified, these conditions lead to the following solutions for \hat{x}_3 and ϕ_3 :

$$\begin{aligned} \hat{x}_3(\tau_1, \tau_2) &= \cos(2\pi\tau_1 + 2\pi f_2\tau_2) \\ \phi_3(t) &= f_0 t + \frac{k}{2\pi} \cos(2\pi f_2 t) - f_2 t. \end{aligned} \quad (11)$$

Although \hat{x}_3 and ϕ_3 are not identical to \hat{x}_2 and ϕ in (6) and (7), they retain the desired property of being easy to sample.

As already noted, when \hat{x}_2 and ϕ in (6) and (7) are chosen to be the warped bivariate representation of $x(t)$, the instantaneous frequency in (4) is the derivative of $\phi(t)$. The derivative of $\phi_3(t)$, on the other hand, differs from the instantaneous frequency by the constant $-f_2$. At first sight, this seems to pose a paradox: different choices of $\phi(t)$ differ in their derivatives; the previous discussion has hinted that this derivative is equal to (or related to) the instantaneous frequency; hence, how can one say for certain what the frequency is at any given instant? The resolution to this lies in the fact that *all choices of $\phi(t)$ that result in compact representations* will differ in their derivatives $(\partial\phi)/(\partial t)$ by amounts only of the order of the slow frequency f_2 . When the fast frequency is much greater than the slow one, this difference is small compared to the instantaneous frequency in (4), therefore, the term *local frequency* for $(\partial\phi)/(\partial t)$ is justified. The utility of the local frequency is that it is concretely defined for *any* FM signal (possibly with nonsinusoidal waveforms and varying amplitudes), not just the ideal one of (3), yet retains the essential intuition of FM. The ambiguity in $(\partial\phi)/(\partial t)$, of order f_2 , is quite reasonable, since the intuitive concept of frequency is only meaningful to the same order. It should be kept in mind, of course, that concepts of varying frequency make intuitive sense only when the fast and slow time scales are widely separated.

The time-warping concept can also be understood in a different, visual, manner. The difficulty in using \hat{x}_1 of (5) is due to the fact that changing t_2 by even a small amount results in a large change in the phase of the outer cosine function, because k is large. Thus, the function is the same on all lines parallel to the t_1 axis, except for a phase that differs substantially for even lines that are nearby. The representation problem that this causes can be dealt with by sliding these lines up and down in the t_1 direction till there is no variation (or slow variation) in the phase from one line to another. This results in changing the rectangular domain box of Fig. 2 to a nonrectangular one, but whose width is *constant* (i.e., with curved but parallel boundaries). In addition, the straight-line $t_1 = t_2$ path changes to a curved path because of the phase adjustment. The doubly periodic bivariate representation can be obtained by tiling the t_1 - t_2 plane with the curved domain boxes (possible because the width is constant); in fact, after extending the function to the entire plane, it is possible to redefine the domain box to be a rectangle once again, resulting in Fig. 5.

The above discussion has summarized our basic strategy for representing FM efficiently; it now remains to concretize these notions in the framework of an arbitrary dynamical system defined by DAEs. This is accomplished in the following section by the WaMPDE, which is a PDE similar to the MPDE, but with a multiplicative factor of $(\partial\phi)/(\partial t)$ modifying one of the differential terms. By solving the WaMPDE together with the phase condition mentioned above, compact representations of the solutions of autonomous systems can be found by efficient numerical methods.

III. WaMPDE

We consider a nonlinear system modeled using vector DAEs, a description adequate for circuits [37] and many other applications

$$\frac{d}{dt} q(x(t)) + f(x(t)) = b(t). \quad (12)$$

In the circuit context, $x(t)$ is a vector of node voltages and branch currents; $q(\cdot)$ and $f(\cdot)$ are nonlinear functions describing the charge/flux and resistive terms, respectively. $b(t)$ is a vector forcing term consisting of inputs, usually independent voltage or current sources.

We now define the $(p+1)$ -dimensional WaMPDE to be

$$\sum_{i=1}^p \left(\omega_i(\tau_{p+1}) \frac{\partial q(\hat{x})}{\partial \tau_i} \right) + \frac{\partial q(\hat{x})}{\partial \tau_{p+1}} + f(\hat{x}) = \hat{b}(\tau_1, \dots, \tau_{p+1}). \quad (13)$$

τ_1, \dots, τ_p are p warped time scales, while τ_{p+1} is an unwarped time scale. Each warped time variable has an associated frequency function $\omega_i(\tau_{p+1})$, which depends on the unwarped time variable. \hat{x} and \hat{b} are multivariate functions of the $p+1$ time variables. These quantities represent generalizations of the concepts introduced in Section II—each warped time corresponds to an independent FM mode of the system, while the unwarped one represents a non-FM time scale. It is straightforward to extend (13) to more than one unwarped time scale.

The utility of (13) lies in its special relationship with (12). Consider any solution \hat{x} of (13), together with the condition

$$b(t) = \hat{b}(\phi_1(t), \dots, \phi_p(t), t), \quad \phi_i(t) = \int_0^t \omega_i(\tau) d\tau. \quad (14)$$

If we define the function $x(t)$ as

$$x(t) = \hat{x}(\phi_1(t), \dots, \phi_p(t), t) \quad (15)$$

then, it is easy to show by substitution that $x(t)$ satisfies (12). Hence, if we can find any solution of (13), we have automatically found one for the original problem, i.e., (12). As explained in Section II, solving the WaMPDE directly for the multivariate functions can be advantageous.

For concreteness in the following, we now specialize to the case when there are only two time variables, and the function b is used directly in (13)

$$\omega(\tau_2) \frac{\partial q(\hat{x})}{\partial \tau_1} + \frac{\partial q(\hat{x})}{\partial \tau_2} + f(\hat{x}(\tau_1, \tau_2)) = b(\tau_2). \quad (16)$$

Corresponding to (14) and (15), specifying

$$x(t) = \hat{x}(\phi(t), t), \quad \phi(t) = \int_0^t \omega(\tau_2) d\tau_2 \quad (17)$$

results in $x(t)$ being a solution to (12).

Next, we describe how (16) can be solved to determine $\hat{x}(\tau_1, \tau_2)$ and $\omega(\tau_2)$. We first assume that $\hat{x}(\tau_1, \tau_2)$ is periodic in τ_1 with period 1

$$\hat{x}(\tau_1, \tau_2) = \sum_{i=-\infty}^{\infty} \hat{X}_i(\tau_2) e^{ji\tau_1}. \quad (18)$$

We note that if $\hat{x}(\tau_1, \tau_2)$ satisfies (16), then so does for $\hat{x}(\tau_1 + \Delta, \tau_2)$, for any $\Delta \in \mathcal{R}$ —this is simply because (16) is au-

tonomous in the τ_1 time scale. We remove this ambiguity in the same way as for unforced autonomous systems, i.e., by fixing the phase of one of the variables to some value,⁴ e.g., 0. This is the phase constraint mentioned in (9).

We expand (16) in 1-D Fourier series in τ_1 , and also include the phase constraint, to obtain

$$\sum_{i=-\infty}^{\infty} \left(\frac{\partial \hat{Q}_i(\tau_2)}{\partial \tau_2} + j i \omega(\tau_2) \hat{Q}_i(\tau_2) + \hat{F}_i(\tau_2) \right) e^{j i \tau_1} = b(\tau_2) \quad (19)$$

$$\Im \left\{ \hat{X}_l^k(\tau_2) \right\} = 0. \quad (20)$$

$\hat{Q}_i(\tau_2)$ and $\hat{F}_i(\tau_2)$ are the Fourier coefficients of $q(\hat{x}(\tau_1, \tau_2))$ and $f(\hat{x}(\tau_1, \tau_2))$, respectively. k and l are fixed integers; $\hat{X}_l^k(\tau_2)$ denotes the l th Fourier coefficient of the k th element of \hat{x} . Here, k is the index of the variable of \hat{x} on which a phase constraint is being applied.

Equations (19) and (20) together form a DAE system which can be solved for isolated solutions. In practice, the Fourier series (19) can be truncated to $N_0 = 2M + 1$ terms with i restricted to $-M, \dots, M$. In this case, (19) and (20) lead to $N_0 + 1$ equations in the same number of unknown functions of τ_2 .

Applying periodic or initial boundary conditions to the DAE system (19) and (20) leads to quasi-periodic or envelope-modulated FM solutions.

A. Quasi-Periodic and Envelope Solutions

Assume $b(t)$ periodic with period T_2 or angular frequency $\omega_2 = (2\pi)/T_2$. Also assume that the solution of (16) is periodic in both arguments, i.e., $\hat{x}(\tau_1, \tau_2)$ is $(1, T_2)$ periodic and $\omega(\tau_2)$ is T_2 periodic. $\omega(\tau_2)$ can then be written as

$$\omega(\tau_2) = \omega_0 + p'(\tau_2) \quad (21)$$

where ω_0 is a constant and $p'(\cdot)$ is a zero-mean T_2 -periodic waveform. Using (21) and (17), we obtain

$$\phi(t) = \omega_0 t + p(t) \quad (22)$$

where $p(t)$ is a T_2 -periodic function.

We motivate these assumptions by showing that such periodic forms for $\hat{x}(\cdot, \cdot)$ and $\omega(\cdot)$ capture FM and AM quasi-periodicity, mode-locking, and period multiplication.

Expand $\hat{x}(\tau_1, \tau_2)$ in the Fourier series

$$\hat{x}(\tau_1, \tau_2) = \sum_{i,k=-\infty}^{\infty} \hat{X}_{i,k} e^{j i \tau_1} e^{j k \omega_2 \tau_2} \quad (23)$$

where the constants $\hat{X}_{i,k}$ are Fourier coefficients. Substituting (23) into (17), we obtain

$$x(t) = \sum_{i,k=-\infty}^{\infty} \hat{X}_{i,k} e^{j i (\omega_0 t + p(t))} e^{j k \omega_2 t}. \quad (24)$$

Consider, for example, the term of (24) with $i = 1$ and $k = 0$

$$\begin{aligned} \hat{X}_{1,0} e^{j(\omega_0 t + p(t))} &= \hat{X}_{1,0} \cos(\omega_0 t + p(t)) \\ &\quad + j \hat{X}_{1,0} \sin(\omega_0 t + p(t)). \end{aligned} \quad (25)$$

⁴or some slow function of τ_2 ; the selection of a slowly-varying phase condition is, in fact, the key to compact numerical representation of $\hat{x}(\cdot, \cdot)$.

When $\omega(t)$ is nontrivially T_2 periodic, $p(t)$ is also nontrivially T_2 periodic. (25) can then readily be recognized to be a frequency-modulated signal with instantaneous frequency $\omega(t)$. Hence the WaMPDE with periodic solutions can capture not only FM signals, but also the more general form of (24).

We now show that various special cases of $\omega(\cdot)$ correspond to physical situations of interest. When $\omega(\cdot)$ is simply some constant ω_0 , i.e., $p'(\cdot) \equiv 0$, then the time-domain solution (24) has no FM, but is AM quasi-periodic with angular frequencies ω_0 and ω_2 . If $\omega_0 = \omega_2$, the response has the same period as the external forcing frequency, and the system is mode locked or entrained. If ω_0 is a submultiple of ω_2 , the period of the response is a multiple of that of the forcing. This phenomenon, period multiplication, is not only often designed for (e.g., in frequency dividing circuits), but is also observed in dynamic systems en route to chaos.

Next, we indicate how (19) and (20), with periodic boundary conditions, can be turned into a set of nonlinear equations for numerical solution⁵. Equations (19) and (20) is discretized at N_1 points along the τ_2 axis, covering the interval $[0, T_1]$. The differentiation operator is replaced by a numerical differentiation formula (e.g., backward Euler or trapezoidal), and when the periodic boundary condition $\hat{X}_i(0) = \hat{X}_i(T_1)$ is applied, a system of $N_1(N_0 + 1)$ nonlinear algebraic equations in $N_1(N_0 + 1)$ unknowns is obtained. This set of equations is solved with any numerical method for nonlinear equations, such as Newton–Raphson or continuation (e.g., [38]), to obtain the solution of the WaMPDE. Further, when iterative linear algebra and factored-matrix methods [5]–[8] are employed, computation and memory requirements grow almost linearly with size, making calculations practical for even large systems.

By applying initial conditions rather than periodic boundary conditions, (19) and (20) can be solved for aperiodic ($\{\hat{X}_i(\tau_2)\}, \omega(\tau_2)$). These envelope-modulated solutions can be useful for investigating transient behavior in systems with FM. To obtain envelope solutions, (19) and (20) are solved by time stepping in τ_2 using any DAE solution method, starting from (say) $\tau_2 = 0$. An initial condition ($\{\hat{X}_i(0)\}, \omega(0)$) is specified. For typical applications, a natural initial condition is the solution of (12) with no forcing, i.e., with $b(t)$ constant. The procedure for discretizing of the WaMPDE for quasi-periodic or time-stepping solutions is similar to that for the MPDE; further details may be found in [2].

IV. APPLICATION

The VCO in Fig. 7 was simulated using numerical techniques derived from the WaMPDE. The oscillator consists of an *LC* tank in parallel with a nonlinear resistor, whose resistance is negative in a region about zero and positive elsewhere. This leads to amplitude-stable oscillations. The capacitance was varied by adjusting the physical plate separation of a novel **Micro Electro Mechanical Structure (MEMS)** varactor with a separate control voltage. The damping parameter of the

⁵We outline a time-domain method for the τ_2 axis, leading to a mixed frequency–time method; purely time-domain or frequency-domain methods are equally straightforward.

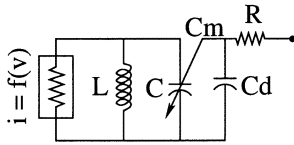


Fig. 7. VCO.

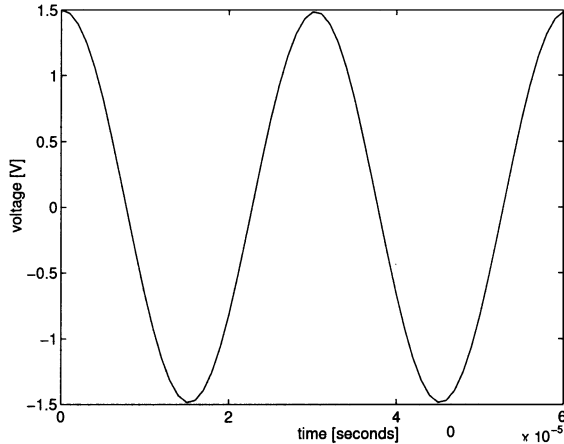


Fig. 8. VCO: controlling voltage

mechanical structure (corresponding to the lowpass RC filter) was initially assumed small, corresponding to a near vacuum.

Representative values of the elements in Fig. 7 are $R = 1 \text{ k}\Omega$, $C_d = 0.3 \text{ }\mu\text{F}$, $C = 1/(2\pi) \text{ }\mu\text{F}$, $C_m = 1/(4\pi) \text{ }\mu\text{F/V}$, and $L = 1/(2\pi) \text{ }\mu\text{H}$. The nonlinear negative-resistance element's current-voltage characteristic was given by

$$i = f(v) = (G_0 - G_\infty) V_k \tanh\left(\frac{v}{V_k}\right) + G_\infty v \quad (26)$$

where $G_0 = -0.1$, $G_\infty = 0.25$, and $V_k = 1$.

An envelope simulation was conducted using purely time-domain numerical techniques for both τ_1 and τ_2 axes. The initial control voltage of 1.5 V resulted in an initial frequency of about 0.75 MHz; Fig. 8 shows the variation of the sinusoidal controlling voltage, with time-period 30 times that of the unforced oscillator. Fig. 9 shows the resulting change in local frequency, which varies by a factor of almost 3.

Fig. 10 depicts the bivariate waveform of the capacitor voltage (i.e., one entry of the vector $\hat{x}(\tau_1, \tau_2)$), with the warped τ_1 axis scaled to the oscillator's nominal time-period of 1 μs . It is seen that the controlling voltage changes not only the local frequency, but also the amplitude and shape of the oscillator waveform.

The circuit was also simulated by time-stepping numerical ODE methods ("transient simulation" in SPICE terminology). The waveform from this simulation, together with the 1-D waveform obtained by applying (15) to Fig. 10, are shown in Fig. 11. The match is so close that it is difficult to tell the two waveforms apart; however, the thickening of the lines at about 60 μs indicates a deviation of the transient result from the WaMPDE solution. FM can be observed in the varying density of the undulations.

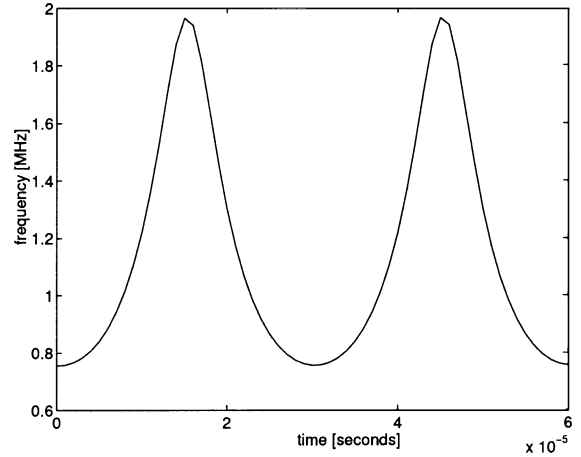


Fig. 9. VCO: FM.

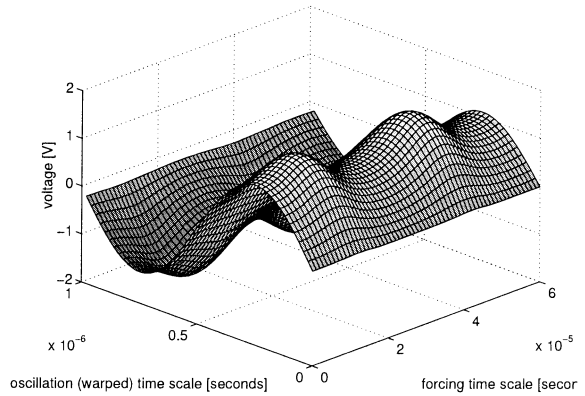


Fig. 10. VCO: bivariate representation of capacitor voltage.

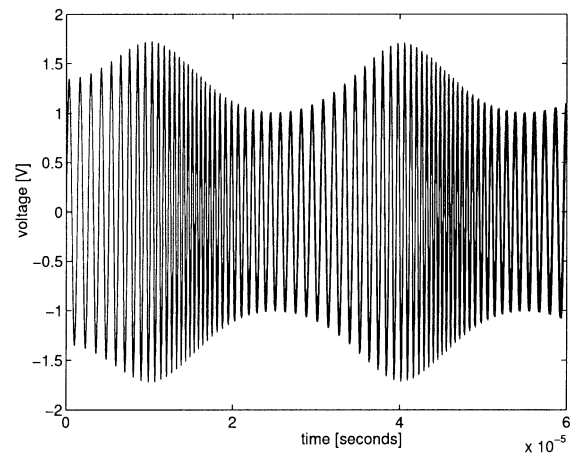


Fig. 11. VCO: WaMPDE versus transient simulation.

The VCO was simulated again after two modifications: the damping of the MEMS varactor was increased to correspond to an air-filled cavity, and the controlling voltage was varied much more slowly, i.e., about 1000 times slower than the nominal period of the oscillator. The controlling voltage was the same sinusoid shown in Fig. 8, but with a period of 1 ms. Fig. 12 shows the new variation in frequency; note the settling behavior and the smaller change in frequency, both due to the slow dynamics of the air-filled varactor.

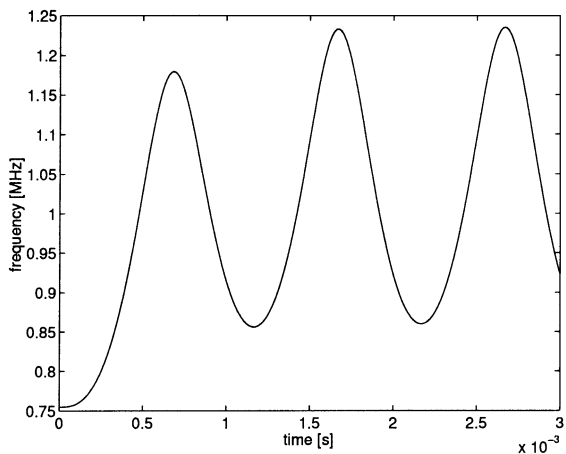


Fig. 12. Modified VCO: FM.

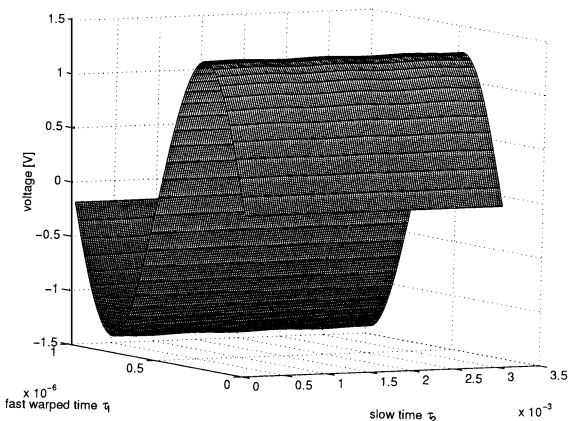


Fig. 13. Modified VCO: bivariate capacitor voltage.

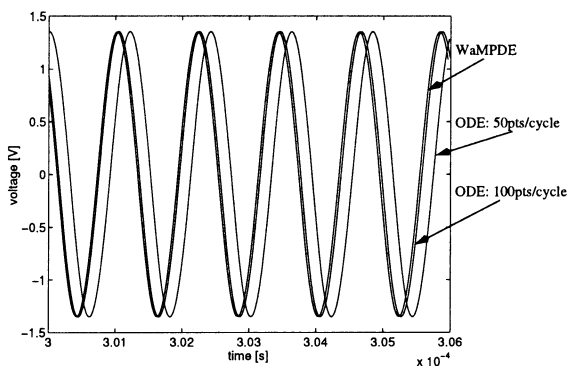


Fig. 14. Modified VCO: WaMPDE versus transient (a few cycles at 10% of the full run; phase errors from transient increase later).

Fig. 13 depicts the new bivariate capacitor voltage waveform. Note that unlike Fig. 10, the amplitude of the oscillation changes very little with the forcing. This was corroborated by transient simulation, the full results of which are not depicted due to the density of the fast oscillations. A small section of the 1-D waveform, consisting of a few cycles around 0.3 ms, is shown in Fig. 14. The 1-D WaMPDE output of (15) is compared against two runs of direct transient simulation, using 50 and 100 points per nominal oscillation period, respectively. It can be seen that even at an early stage of the simulation, direct

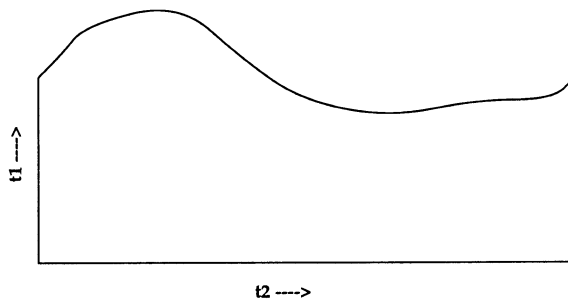


Fig. 15. Moving boundaries cannot generate steady-state solutions.

transient simulation with 50 points per cycle builds up significant phase error. This is reduced considerably when 100 points are taken per cycle, but further along (not shown), the error accumulates again, reaching many multiples of 2π by the end of the simulation at 3 ms. In contrast, the WaMPDE achieves much tighter control on phase because the phase condition (a time-domain equivalent of (20)) explicitly prevents build-up of error. To achieve accuracy comparable to the WaMPDE, transient simulation required 1000 points per nominal cycle, with a resulting speed disadvantage of two orders of magnitude.

V. CONCLUSION

We have presented a multitime equation formulation useful for oscillatory systems. The approach generalizes the MPDE [1], [2] by applying time-warping functions to represent frequency-modulated signals efficiently. A local frequency variable appears explicitly in the resulting MPDEs, which we dub the WaMPDE. The WaMPDE can be used as a starting point for analysis and simplification of oscillator equations if they are available in closed form. It can also be applied to obtain numerical methods that provide new capabilities and are more accurate and efficient than existing techniques.

Other applications of the WaMPDE, being investigated currently, include perturbation and noise analysis of oscillators. The concept of warped time has also been expanded to obtain more general forms of the WaMPDE. It is possible that further understanding of complex phenomena in oscillators and other dynamical systems may result from new applications and generalizations.

APPENDIX CURVED BOUNDARIES AND FM

For simplicity, assume a two-rate state-equation form for the MPDE of a forced oscillator

$$\frac{\partial \hat{x}}{\partial t_1} + \frac{\partial \hat{x}}{\partial t_2} = f(\hat{x}) + \hat{b}(t_1, t_2). \quad (27)$$

Assume that t_2 is the slow time scale, t_1 is the fast time scale, and that \hat{b} is independent of t_1 , as is reasonable for a forced oscillator. Now assume that this system can be solved for periodic solutions on a moving boundary in the t_1 direction, given by the scalar function $T_1(t_2)$, which is T_2 periodic (see Fig. 15). This is equivalent to assuming the solution to be in the form

$$\hat{x}(t_1, t_2) = \hat{z} \left(\frac{t_1}{T_1}, \frac{t_2}{T_2(t_1)} \right), \quad \hat{z} \text{ is } (1,1) \text{ periodic.} \quad (28)$$

Now expand the partial differentiation terms of (27) using (28)

$$\frac{\partial \hat{x}}{\partial t_2} = \frac{1}{T_2} \partial_1 \hat{z} \left(\frac{t_2}{T_2}, \frac{t_1}{T_1(t_2)} \right) - \partial_2 \hat{z} \left(\frac{t_2}{T_2}, \frac{t_1}{T_1(t_2)} \right) \underbrace{\frac{t_1}{T_1^2(t_2)}}_{\text{secular term}} \frac{dT_1}{dt_2}(t_2) \quad (29)$$

$$\frac{\partial \hat{x}}{\partial t_1} = \frac{1}{T_1(t_2)} \partial_2 \hat{z} \left(\frac{t_2}{T_2}, \frac{t_1}{T_1(t_2)} \right). \quad (30)$$

Note that (29) contains a so-called *secular term* [23], i.e., a term that increases linearly with t_1 if $T_1(t_2)$ is not a constant. Note further that all other terms of (27) are of the form of (28), i.e., periodic, whereas the secular term increases unboundedly with t_1 . Therefore, no solution of the form of (28) can exist, unless $T_1(t_2)$ is independent of t_2 (i.e., rectangular boundaries). A similar argument can be used to establish that even the DAE of the forced oscillator cannot admit solutions of the type $\hat{x}(t, t)$, with \hat{x} in the form (28). This conclusion is also physically reasonable, for the secular term would imply that the instantaneous frequency of the signal grows unboundedly, which is unphysical.

APPENDIX GENERALIZED WaMPDE FORMS

The WaMPDE (13) is a special case of more general MPDE forms. In this section, we outline these more general forms.

Let d be an integer number of artificial time scales. Define “phase functions” $\hat{\Phi}$ as

$$\hat{\Phi}(t_1, \dots, t_d) = \begin{pmatrix} \tau_1 \\ \vdots \\ \tau_d \end{pmatrix} = \begin{pmatrix} \hat{\phi}_1(t_1, \dots, t_d) \\ \vdots \\ \hat{\phi}_d(t_1, \dots, t_d) \end{pmatrix}. \quad (31)$$

Also define “local frequency” functions $\hat{\Omega}$ to be

$$\hat{\Omega}(\tau_1, \dots, \tau_d) = \begin{pmatrix} \hat{\omega}_1(\tau_1, \dots, \tau_d) \\ \vdots \\ \hat{\omega}_d(\tau_1, \dots, \tau_d) \end{pmatrix}. \quad (32)$$

Let $\hat{\Phi}$ and $\hat{\Omega}$ be related by

$$\left(\frac{\partial}{\partial t_1} + \dots + \frac{\partial}{\partial t_d} \right) \hat{\Phi}(t_1, \dots, t_d) = \hat{\Omega}(\hat{\Phi}(t_1, \dots, t_d)). \quad (33)$$

Note that (33) is a nonlinear PDE, akin to an ODE (as opposed to a DAE) in the sense that the left-hand side is the differentiation of the unknown vector $\hat{\Phi}$. This relation is a generalization phase to the local-frequency relationship (14).

Based on the above, we define a general MPDE form for (12) to be

$$\left[\hat{\Omega}(t_1, \dots, t_d) \cdot \left[\frac{\partial}{\partial t_1}, \dots, \frac{\partial}{\partial t_d} \right] \right] q(\hat{x}(t_1, \dots, t_d)) + f(\hat{x}(t_1, \dots, t_d)) = \hat{b}(t_1, \dots, t_d). \quad (34)$$

Next, we prove a key theorem: that if $\hat{\Omega}$ and \hat{x} together constitute a solution of (34), then $x(t) = \hat{x}(\hat{\Phi}(t, \dots, t))$ solves (12), if $b(t) = \hat{b}(\hat{\Phi}(t, \dots, t))$.

Proof:

$$\begin{aligned} \dot{q}(x(t)) &= \frac{\partial q(\hat{x}(\hat{\Phi}(t, \dots, t)))}{\partial t} \\ &= \frac{\partial q(\hat{x}(t_1 = \phi_1, \dots, t_d = \phi_d))}{\partial t_1} \frac{\partial \phi_1(t, \dots, t)}{t} + \dots \\ &\quad + \frac{\partial q(\hat{x}(t_1 = \phi_1, \dots, t_d = \phi_d))}{\partial t_d} \frac{\partial \phi_d(t, \dots, t)}{\partial t}. \end{aligned}$$

This can be written as a matrix-vector product

$$\dot{q}(x(t)) = \left[\frac{\partial \hat{q}}{\partial t_1}, \dots, \frac{\partial \hat{q}}{\partial t_d} \right] \Big|_{\hat{\Phi}(t, \dots, t)} \begin{bmatrix} \frac{\partial \phi_1}{\partial t} \\ \vdots \\ \frac{\partial \phi_d}{\partial t} \end{bmatrix}.$$

Now, each component of the vector above can be expanded using the chain rule as

$$\begin{aligned} \frac{\partial \phi_k(t, \dots, t)}{\partial t} &= \frac{\partial \phi_k(\tau_1 = t, \dots, \tau_d = t)}{\partial \tau_1} + \\ &\quad + \frac{\partial \phi_k(\tau_1 = t, \dots, \tau_d = t)}{\partial \tau_d} \end{aligned}$$

hence the vector itself is

$$\begin{bmatrix} \frac{\partial \phi_1}{\partial t} \\ \vdots \\ \frac{\partial \phi_d}{\partial t} \end{bmatrix} = \left(\frac{\partial}{\partial \tau_1} + \dots + \frac{\partial}{\partial \tau_d} \right) \hat{\Phi}(t, \dots, t)$$

which, using (33), becomes

$$\begin{bmatrix} \frac{\partial \phi_1}{\partial t} \\ \vdots \\ \frac{\partial \phi_d}{\partial t} \end{bmatrix} = \hat{\Omega}(\hat{\Phi}(t, \dots, t)).$$

Hence, we have

$$\dot{q}(x(t)) = \left[\frac{\partial \hat{q}}{\partial t_1}, \dots, \frac{\partial \hat{q}}{\partial t_d} \right] \Big|_{\hat{\Phi}(t, \dots, t)} \hat{\Omega}(\hat{\Phi}(t, \dots, t))$$

which is simply the first term of (34) evaluated at $(t_1, \dots, t_d) = \hat{\Phi}(t, \dots, t)$. Hence, using (34), we have

$$\begin{aligned} \dot{q}(x(t)) &= -f(\hat{x}(\hat{\Phi}(t, \dots, t))) + b(\hat{x}(\hat{\Phi}(t, \dots, t))) \\ &= -f(x(t)) + b(t) \end{aligned}$$

which proves the assertion. \blacksquare

ACKNOWLEDGMENT

The authors are grateful to the third anonymous reviewer for a thorough examination of the manuscript and detailed suggestions for its improvement.

REFERENCES

- [1] H. G. Brachtendorf, G. Welsch, R. Laur, and A. B. Gerstner, “Numerical steady state analysis of electronic circuits driven by multi-tone signals,” in *Electrical Engineering*. New York: Springer-Verlag, 1996, vol. 79, pp. 103–112.
- [2] J. Roychowdhury, “Analyzing circuits with widely-separated time scales using numerical PDE methods,” *IEEE Trans. Circuits. Syst.*, vol. 48, pp. 578–594, May 2001.

- [3] H. W. Broer, G. B. Huitema, and M. B. Sevryuk, *Quasi-Periodic Motions in Families of Dynamical Systems: Order Amidst Chaos*. New York: Springer-Verlag, 1996.
- [4] A. E. Siegman, *Lasers*. New York: University Science Books, 1986.
- [5] Y. Saad, *Iterative Methods for Sparse Linear Systems*. PWS, MA, 1996.
- [6] R. W. Freund, "Reduced-Order modeling techniques based on krylov subspaces and their use in circuit simulation," Bell Laboratories, Murray Hill, NJ, Tech. Rep. 11 273-980 217-02TM, 1998.
- [7] M. Rösch and K. J. Antreich, "Schnell stationäre simulation nichtlinearer schaltungen im frequenzbereich," (*AEU*) *Elektr. Übertragung*, vol. 46, no. 3, pp. 168–176, 1992.
- [8] P. Feldmann, R. C. Melville, and D. Long, "Efficient frequency domain analysis of large nonlinear analog circuits," in *Proc. IEEE Custom Integrated Circuits Conf.*, May, 5–8 1996, pp. 461–464.
- [9] G. D. Vendelin, *Design of Amplifiers and Oscillators by the S-Parameter Method*. New York: Wiley, 1982.
- [10] I. M. Parzen, *Design of Crystal and Other Harmonic Oscillators*. New York: Wiley, 1983.
- [11] U. Rohde and , *Microwave and Wireless Synthesizers: Theory and Design*. New York: Wiley, 1997.
- [12] I. M. Gottlieb, *Practical Oscillator Handbook*. New York: Oxford, 1997.
- [13] M. Farkas, *Periodic Motions*. New York: Springer-Verlag, 1994.
- [14] C. Hayashi, *Nonlinear Oscillations in Physical Systems*. New York: McGraw-Hill, 1964.
- [15] H. Haaken, *Advanced Synergetics*. New York: Springer-Verlag, 1987.
- [16] J. A. Murdock, *Perturbations: Theory and Methods*. New York: Wiley, 1991.
- [17] A. Nayfeh and D. Mook, *Nonlinear Oscillations*. New York: Wiley, 1979.
- [18] B. van der Pol, "On oscillation hysteresis in a simple triode generator," *Phil. Mag.*, vol. 43, pp. 700–719, 1922.
- [19] T. S. Parker and L. O. Chua, *Practical Numerical Algorithms for Chaotic Systems*. New York: Springer-Verlag, 1989.
- [20] A. Nayfeh and B. Balachandran, *Applied Nonlinear Dynamics*. New York: Wiley, 1995.
- [21] E. N. Lorenz, "Deterministic nonperiodic flow," *J. Atmos. Sci.*, vol. 20, pp. 130–141, 1963.
- [22] L. O. Chua, "The genesis of Chua's circuit," (*AEU*) *Arch. Elektr. Übertragung*, vol. 46, pp. 248–291, 1992.
- [23] J. Kevorkian and J. D. Cole, *Perturbation Methods in Applied Mathematics*. New York: Springer-Verlag, 1981.
- [24] R. Mickens, *Oscillations in Planar Dynamic Systems*. Singapore: World Scientific, 1995.
- [25] L. W. Nagel, "SPICE2: A Computer Program to Simulate Semiconductor Circuits," Ph.D. dissertation, Elec. Res. Lab., EECS Dept., Univ. of California, Berkeley, CA, 1975.
- [26] T. L. Quarles, *SPICE 3C.1 User's Guide*. Berkeley, CA: Univ. of California, Apr. 1989, p. 94 720.
- [27] T. J. Aprille and T. N. Trick, "Steady-state analysis of nonlinear circuits with periodic inputs," *Proc. IEEE*, vol. 60, pp. 108–114, Jan. 1972.
- [28] S. Skelboe, "Computation of the periodic steady-state response of nonlinear networks by extrapolation methods," *IEEE Trans. Circuits. Syst.*, vol. CAS-27, pp. 161–175, Mar. 1980.
- [29] R. Telichevesky, K. Kundert, and J. White, "Efficient steady-state analysis based on matrix-free Krylov subspace methods," in *Proc. IEEE Decision and Control*, vol. 1, 1995, pp. 480–484.
- [30] M. S. Nakhla and J. Vlach, "A piecewise harmonic balance technique for determination of periodic responses of nonlinear systems," *IEEE Trans. Circuits. Syst.*, vol. CAS-23, p. 85, Jan. 1976.
- [31] S. A. Haas, *Nonlinear Microwave Circuits*. Norwood, MA: Artech House, 1988.
- [32] V. Rizzoli and A. Neri, "State of the art and present trends in nonlinear microwave CAD techniques," *IEEE Trans. Microwave Theory Tech.*, vol. 36, pp. 343–365, Feb. 1988.
- [33] K. S. Kundert, J. K. White, and A. Sangiovanni-Vincentelli, *Steady-State Methods for Simulating Analog and Microwave Circuits*. Norwell, MA: Kluwer, 1990.
- [34] R. J. Gilmore and M. B. Steer, "Nonlinear circuit analysis using the method of harmonic balance—A review of the art. Part I. Introductory concepts," *Int. J. Microwave Millimeter Wave CAE*, vol. 1, no. 1, 1991.
- [35] M. Rösch, "Schnell Simulation des stationären Verhaltens nichtlinearer Schaltungen," Ph.D. dissertation, Technischen Univ. München, Munich, Germany, 1992.
- [36] H. G. Brachtendorf and R. Laur, "Transient simulation of oscillators," Bell Labs, Murray Hill, NJ, Tech. Rep. ITD-98-34 096K, 1998.
- [37] L. O. Chua and P.-M. Lin, *Computer-Aided Analysis of Electronic Circuits: Algorithms and Computational Techniques*. Englewood Cliffs, NJ: Prentice-Hall, 1975.
- [38] E. L. Allgower and K. Georg, *Numerical Continuation Methods*. New York: Springer-Verlag, 1990.

Onuttom Narayan, photograph and biography not available at the time of publication.



Jaijeet Roychowdhury received the Bachelor's degree in electrical engineering from the Indian Institute of Technology, Kanpur, India, in 1987, and the Ph.D. degree in electrical engineering and computer science from the University of California, Berkeley, in 1993.

From 1993 to 1995, he was with the CAD Lab, AT&T Bell Laboratories, Allentown, PA. From 1995 to 2000, he was with the Communication Sciences Research Division, Lucent Technologies, Bell Laboratories, Murray Hill, NJ. From 2000 to 2001, he was with CeLight, Inc., an optical networking startup, Silver Springs, MD. Since 2001, he has been with the Electrical and Computer Engineering Department and the Digital Technology Center of the University of Minnesota, Minneapolis. His professional interests include the design, analysis, and simulation of electronic, electrooptical, and mixed-domain systems, particularly for high-speed and high-frequency communications.

Dr. Roychowdhury received the Distinguished or Best Paper Awards at ICCAD 1991, DAC 1997, ASP-DAC 1997, and ASP-DAC 1999, and was cited for Extraordinary Achievement by Bell Laboratories.